Calculations of the screened self-energy and vacuum polarization in Li-like, Na-like, and Cu-like ions

Steven A. Blundell

Département de Recherche Fondamentale, LI2A, Centre d'Etudes Nucléaires de Grenoble, Boîte Postale 85X, F-38041 Grenoble CEDEX, France

We present *ab initio* calculations of the screened self-energy and vacuum polarization for the resonance transitions of Li-like, Na-like, and Cu-like ions, for a degree of ionization of about 10 or greater. The direct part of the Dirac-Fock potential is incorporated to all orders in the radiative corrections, and exchange effects are added in leading order. When combined with previous calculations of correlation and nuclear effects, our results agree with experiment at the level of experimental uncertainty with only a few exceptions, most notably the low-Z part of the Cu isoelectronic sequence. The calculations agree well at low Z with phenomenological estimates of the QED terms based on scalings of the known hydrogenic values but deviate slightly at high Z. We discuss the leading omitted two-photon QED terms.

PACS number(s): 31.20.Tz, 12.20.Ds, 31.30.Jv

I. INTRODUCTION

The calculation of radiative corrections in many-electron systems is an outstanding problem in theoretical atomic physics. The need for rigorous calculations has been highlighted by the development of high-precision spectroscopy for ions of increasingly high charge state. For example, Schweppe et al. [1] have measured the resonance transition in Li-like U with an accuracy of 0.1 eV, about 0.2% of the radiative corrections to the transition energy, and comparable accuracy has been achieved by Cowan et al. [2] in Na-like Pt ($Z = 78$), and by Seely et al. [3] in high-Z Cu-like systems. A partial theoretical treatment of such measurements is provided by relativistic many-body perturbation theory (RMBPT), which Johnson, Blundell, and Sapirstein [4–7] have used to calculate highly converged relativistic correlation and Breit corrections for one-valence-electron ions. However, the estimation of the large QED contributions to the spectra has in most cases relied on scaling the accurately known hydrogenic values through plausible, though strictly untested, phenomenological prescriptions. An *ab initio* calculation of the many-electron QED terms allows one to use the experiments to test the bound-state QED formalism itself rather than to test theoretical approximation schemes. Since for high-Z ions the intense nuclear Coulomb field must be included nonperturbatively in the radiative corrections, such a test of QED complements the many existing tests in weak external fields, such as the "$g - 2$" experiment, the hyperfine structure of muonium, or the QED terms of neutral helium.

In this paper we present a rigorous evaluation of a subset of QED terms that, when combined with RMBPT energies, agrees well with experiment for one-valence-electron ions over a large range of the Periodic Table, from ions with a degree of ionization of about 10, the lowest Z value we calculate, up to $Z = 92$. The agreement with experiment is within one to two experimental standard deviations with only a few exceptions, most notably the Cu isoelectronic sequence at low Z. We speculate that here the disagreement is due to missing high-order correlation diagrams.

Until recently, precise values for the self-energy in excited states of high-Z ions were known only for point-nucleus hydrogenic systems through the work of Mohr [8–10] and Mohr and Kim [11]. Here we wish to consider the modification, or "screening," of the hydrogenic QED terms in many-electron systems due to correlation effects. A possible approach to this problem is to use perturbation theory, expanding about the bare nuclear potential $V_{\rm nuc}(r)$ and treating the entire electron-electron interaction as a perturbation [12]. This perturbation series, however, converges rapidly only for few-electron systems at high Z, for which the electronic mean field $V_{\rm scrn}(r)$ is small compared to the nuclear Coulomb field. Although such systems provide some of the most interesting tests of QED in intense fields, we wish here to consider as well ions in which the number of core electrons N is a large fraction of the nuclear charge Z. Then, as we will see, convergence of perturbation theory improves significantly if the perturbation series is developed instead about a "reference potential" $V(r) = V_{\rm nuc}(r) + V_{\rm scrn}(r)$.

To adopt this second approach, we require an algorithm for evaluating the lowest-order self-energy in a general potential $V(r)$. Since the screening potential $V_{\rm scrn}(r)$ is ideally some form of self-consistent potential defined numerically on a radial grid, one cannot make use of the special analytic properties of the Coulomb potential that have led to such high accuracy for hydrogenic ions. A fully numerical procedure for a general potential has been developed by Cheng, Johnson, and Sapirstein [13], who extended the algorithm of Brown, Langer, and Schaefer [14]. This algorithm suffers, however, from a quite slowly converging partial-wave expansion with asymptotic form $1/L^2$. After taking the partial-wave expansion to $L \sim 100$, already hard for a numerically defined potential, Cheng, Johnson, and Sapirstein [13] still achieved

a numerical precision worse than the best experimental precision at high Z.

A central feature of the present work is a recently introduced algorithm [15–17] for evaluating the self-energy in an arbitrary local potential, which has an improved partial-wave convergence as $1/L^3$. As shown in [17], this more rapid L convergence, combined with a cancellation of the high-L contributions in a transition, permits calculation of the lowest-order self-energy in a transition with a numerical precision of at worst 0.003 eV for $Z > 70$, much better than the best experimental precision at high Z. We use this technique for low Z also, finding a numerical precision that becomes comparable to the experimental precision at a degree of ionization of about ten. By a suitable choice of $V_{scrn}(r)$, we can account for the bulk of the screening effect, as was done in Ref. [13]. We consider also other screening effects that can be expressed as off-diagonal matrix elements of the self-energy or vacuum polarization.

By comparing the *ab initio* self-energy with the scaled hydrogenic value for a given model potential, we can also test quantitatively the phenomenological schemes commonly used to obtain screened QED corrections. Such schemes can be usefully incorporated in production codes for problems where high precision is not so important. Most existing schemes follow the prescription of scaling the hydrogenic QED according to the probability density at the origin, or through some closely related procedure. Our results show that these methods give excellent approximations for s states for low to medium Z. At $Z = 92$, the deviations are small, though just significant at the level of experimental error for Li-like U.

The paper is organized as follows. In Sec. II we describe the subset of Feynman diagrams included in our treatment of QED screening. Numerical results are given in Sec. III, and compared to experiment and other calculations. Section IV discusses the dependence of the QED screening on the normalization at the origin. Finally, in the conclusions, we discuss the prospects for evaluating omitted QED terms and speculate on their likely size.

II. FORMALISM

A QED perturbation expansion about a general reference potential $V(r)$ may be developed by adopting a Furry representation of QED in the potential $V(r)$ and applying, for example, the theorem of Gell-Mann and Low [18–20]. As discussed in [21], this perturbation theory contains consistently both the relativistic correlation terms of RMBPT and the radiative corrections of interest here. Our QED treatment is then a natural extension of the RMBPT work, which we now briefly describe.

In their RMBPT method [4–7], Johnson, Blundell, and Sapirstein considered only the correlation-type Feynman diagrams in which photons are exchanged from one atomic electron to another. They chose the potential $V_{scrn}(r)$ to be the nonlocal V^{N-1} Dirac-Fock potential for the core, $V_{DF}(r)$. For the photon propagator, they used Coulomb gauge and neglected the frequency dependence, that is, set k_0 in the momentum-space representation (see the Appendix) equal to zero. For the electron propaga-

tor, they neglected negative-energy electron states in the spectral decomposition. The resulting perturbation series generalizes the nonrelativistic one by replacing the Coulomb interaction with the sum of the Coulomb and Breit interactions, and by replacing Schrödinger electron states with Dirac states belonging to the positive-energy branch of the spectrum. This perturbation series can also be thought of as arising in the "no-pair" approximation of Sucher [22], using the Dirac-Coulomb-Breit many-electron Hamiltonian projected on to positive-energy states. Johnson, Blundell, and Sapirstein evaluated terms up to third order in the Coulomb interaction, as well as the first-order Breit interaction, and second-order terms with one Breit and one Coulomb interaction. They also evaluated the frequency-dependent part of the one-photon exchange diagram, and estimated the small nuclear recoil effect by using the nonrelativistic nuclear-kinetic-energy operator. The effects they omitted, then, include the self-energy and vacuum polarization, as well as the neglected negative-energy effects, and the photon-frequency-dependent (retardation) effects in two-photon diagrams.

We now turn to the self-energy and vacuum polarization, given in lowest order by the Feynman diagrams in Fig. 1. The "screening" corrections to these effects are given in lowest order by diagrams in which an additional photon is exchanged with another atomic electron. Let us consider initially the perturbation expansion about the bare nuclear Coulomb potential, in which the entire electron-electron interaction forms the perturbation. The first-order screening corrections are then given by the diagrams in Fig. 2. [Note that we have not shown explicitly a set of "energy correction" or "derivative" terms that make the vertex-correction diagrams 2(b), 2(f), 2(j), and 2(m) finite [12].] We classify these diagrams according to whether the radiative correction acts on a *valence* line [diagrams 2(a)–2(h)] or a *core* line [diagrams 2(i)–2(n)]. The valence screening terms dominate, but the core terms, which represent the relaxation of the core during the transition, are also significant. A further classification is into *direct* effects [diagrams 2(a)–2(d) and 2(i)–2(k)] and *exchange* effects [diagrams 2(e)–2(h) and 2(l)–2(n)], according to the relative alignment of the ingoing and outgoing states.

First we consider the direct valence screening terms 2(a)–2(d). Explicit calculation shows the sum of diagrams 2(a) and 2(b) to be roughly N/Z times the lowest-
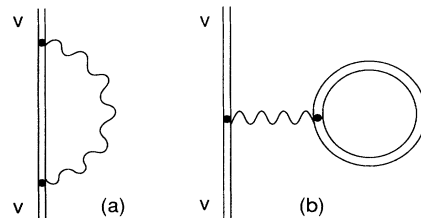

FIG. 1. Feynman diagrams for the lowest-order bound-state (a) self-energy and (b) vacuum polarization. v is the valence state.
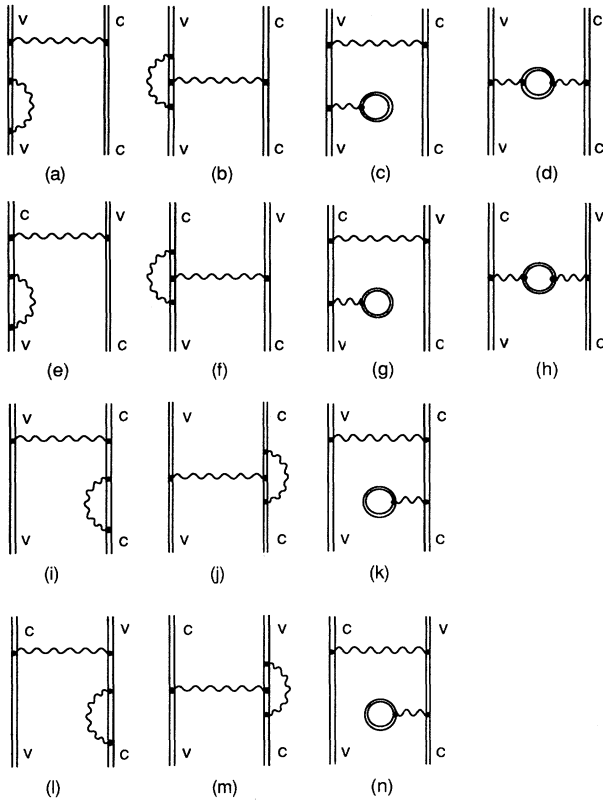
FIG. 2. Feynman diagrams for first-order screening effects on the self-energy and vacuum polarization in a one-valence-electron system. v is the valence state; c is the core state. Diagrams lacking symmetry about a horizontal line, e.g., Fig. 2(a) but not Fig. 2(b), are accompanied by their mirror-image counterpart. Counterterms needed to make these diagrams finite are not shown, nor are the "energy-correction" terms that make the vertex-correction terms finite.

order self-energy, where N is the number of core electrons; the vacuum-polarization diagrams 2(c) and 2(d) are a similar fraction of the lowest-order vacuum polarization. Thus for U^{90+} ($Z = 92$, $N = 2$), the diagrams give a 3% reduction of the lowest-order radiative corrections, while for Bi^{55+} ($Z = 83$, $N = 28$) we find a much larger reduction, about 40%. In the former example, this perturbative treatment is probably adequate, since second-order direct screening effects are expected to be of order 0.03^2 times the lowest-order effect, that is, about

one-half of an experimental standard deviation. In the latter example, however, the corresponding estimate suggests a second-order correction of about 35 experimental standard deviations. This simple type of estimate of the likely size of second-order corrections gives results larger than the experimental error for most of the Na-like and Cu-like measurements considered here, and for the low-Z Li-like measurements.

In these latter cases, it is useful to sum an infinite sequence of screening diagrams, which can be done conveniently by modifying the potential used to calculate the lowest-order radiative corrections. We separate the V^{N-1} Dirac-Fock potential into local direct and nonlocal exchange parts, $V_{DF} = V_{DF,dir} + V_{DF,ex}$, and use the direct part in the lowest-order radiative corrections, taking $V(r) = V_{nuc}(r) + V_{DF,dir}(r)$. In this way, diagrams 2(a)–2(d) are effectively absorbed into the lowest-order diagrams of Fig. 1, together with an infinite subset of higher-order diagrams in which the core line is inserted in all ways to all orders in the internal and external lines of the lowest-order radiative corrections. An alternative way of expressing this is to consider $V(r)$ above as the reference potential for the perturbation series. Then, as discussed in Ref. [21], the screening diagrams of Fig. 2 must be supplemented by extra diagrams involving a "potential counterterm" $-V_{DF}(r)$. These extra terms have the effect of canceling diagrams 2(a)–2(d). After this shift of reference potential, the first-order screening effects consist of only the core and exchange terms, 2(e)–2(n).

The direct core terms Fig. 2(i)–2(k) can be evaluated by adding a suitable "valence potential" to the potential experienced by a core electron. This approach is described in detail in Ref. [17].

We next consider the exchange diagrams where the additional photon is attached to the *external* leg of the self-energy or vacuum polarization [Figs. 2(e), 2(g), 2(l), and 2(n)]. We refer to these diagrams as external exchange diagrams. They reduce to off-diagonal matrix elements of the self-energy or vacuum polarization operator. For example, Fig. 2(e) may be expressed as

$$\Delta E^{(e)} = 2 \operatorname{Re} \langle v | \gamma_0 [\Sigma(\varepsilon_v) - \delta m] | \phi \rangle, \tag{1}$$

where $\Sigma(\varepsilon_v)$ is the bound-state self-energy operator, δm is the mass counterterm, and

$$|\phi\rangle = -\alpha \sum_{\substack{i,v \\ (i \neq v)}} \frac{|i\rangle}{\varepsilon_v - \varepsilon_i} \sum_{c\,(\text{core})} \langle ic | (\alpha_\mu)_1 (\alpha_\nu)_2 D^{\mu\nu}(\varepsilon_v - \varepsilon_c; 12) | cv \rangle, \tag{2}$$

and $D^{\mu\nu}(\varepsilon_v - \varepsilon_c; \mathbf{r}_1, \mathbf{r}_2)$ is the photon propagator in the mixed representation [17]. We use the same reference potential $V(r) = V_{nuc}(r) + V_{DF,dir}(r)$ for the electron states that we use for the lowest-order radiative corrections. The Appendix shows that (1) is finite for an arbitrary state $|\phi\rangle$, and that it is gauge invariant over covariant

gauges (but not Coulomb gauge as well). The numerical evaluation of an off-diagonal self-energy follows a simple generalization of the technique for a diagonal self-energy. Expressions for (1) and (2) after angular integration are also given in the Appendix.

The remaining screening diagrams are the *internal* ex-

change diagrams, 2(f), 2(h), and 2(m), in which the additional photon enters the internal loop of the self-energy or vacuum polarization. Grouped with these terms are "energy-correction" terms that make them finite [12]. The internal exchange effects cannot be obtained simply in terms of the lowest-order self-energy or vacuum polarization operators, and require separate consideration that we leave for future work. However, a key result of this paper is the observation that the external exchange screening improves agreement with experiment to the level of an experimental standard deviation in most cases (see Sec. III). This provides some inference that the omitted internal exchange screening terms are small at the level of experimental accuracy. This point is discussed further in the conclusions.

As mentioned above, in perturbation theory about a reference potential $V(r) = V_{\mathrm{nuc}}(r) + V_{\mathrm{DF,dir}}(r)$, the first-order screening is described by just the core and exchange effects in Figs. 2(e)–2(n). The explicit numerical evaluation in Sec. III shows that these terms are quite small, of order $1/Z$ times the lowest-order effect. For medium to large N, the direct valence terms 2(a)–2(d) thus dominate the core and exchange diagrams 2(e)–2(n). For the direct valence terms, the core states tend to contribute coherently to the classical core screening potential. The exchange terms, on the other hand, are suppressed by the angular factor, and further by an overlap integral between core and valence states. The core terms are suppressed by the large excitation energy for core states. With the reference potential $V(r)$ above, second-order screening consists of second-order exchange effects, or combinations of core and exchange effects. A rough estimate of their likely size is β^2 times the lowest-order effect, where β is the ratio of first-order exchange or core terms to lowest-order effects. Such an estimate is below the experimental error for all transitions studied. While not rigorous, this estimate does show that the shift of reference potential produces an improvement in the convergence of perturbation theory that is significant for systems with large N/Z. The improved convergence is least satisfactory for low Z. For higher precision work at low Z, especially for lower Z values than those considered here, it may be important to incorporate exchange or core screening effects to higher order. We have avoided including exchange effects in the reference potential $V(r)$, however, because in addition to destroying gauge invariance in each order of perturbation theory, a nonlocal reference potential spoils the formal cancellation of divergences used in the self-energy algorithm.

Although the use of a different potential $V(r)$ for the RMBPT terms and the radiative corrections is inconsistent, the discussion of the preceding paragraph implies that the sum of all-order direct screening and first-order exchange screening approximates the "self-energy for a Dirac-Fock potential" well for those transitions considered. In future more-precise work, one should perhaps calculate all parts of the QED perturbation series consistently in the same reference potential $V(r)$.

Finally, we make the approximation for the lowest-order vacuum polarization of evaluating rigorously only the dominant Uehling term [23, 24, 17]. For the small

remaining Wichmann-Kroll (WK) terms, we use the hydrogenic value [25] scaled in the same ratio by which the Uehling term scales. This phenomenological modification seems justified in view of the discussion of screening in Sec. IV, although the resulting screening correction to the WK terms is negligible compared with the experimental uncertainty for all transitions considered. In the exchange and core vacuum polarization diagrams of Fig. 2, we neglect the WK terms entirely.

III. NUMERICAL RESULTS

As a preliminary, we give in Table I detailed examples for two particularly accurate high-Z measurements on Li-like U [1] and Na-like Pt [2]. For Li-like U, the RMBPT value includes a gross finite-nuclear-size contribution based on the nuclear parameters of Zumbro et al. [26]; the accuracy of these parameters implies a negligible uncertainty in the transition energy [7]. The RMBPT also includes a nuclear polarization contribution [27]. For Li-like U, the valence self-energy incorporates a finite-nuclear-size correction of 0.80(1) eV and a direct screening correction of 1.77(1) eV [17]. The valence Uehling term incorporates a finite-nuclear-size correction of -0.76 eV and a direct screening correction of -0.44 eV, in precise agreement with [28] and [13], respectively. Note that we treat the core terms in a slightly different way for the two ions. For Li-like ions, we evaluate Figs. 2(i) and 2(j) as described in [17]. For Na-like (and Cu-like) ions, we neglect 2(j) and evaluate 2(i) together with 2(l) as an off-diagonal self-energy (1) with a suitable wave packet $|\phi\rangle$. The small "higher-order" (HO) term represents the two-loop radiative corrections for the hydrogenic ion to lowest order in $Z\alpha$ [28–30].

The results in Table I show some interesting features. The valence exchange screening, Figs. 2(e) and 2(g), has the same sign as the valence direct screening, Figs. 2(a) and 2(c), although for energies the direct and exchange contributions have opposite signs. The sign of the QED corrections follows those of the changes in the normalization at the origin as the direct and exchange Dirac-Fock potentials are added to the valence Hamiltonian. Test calculations show that local Slater-type approximations to exchange, although reproducing the exchange energy, can give the opposite sign for the change in normalization at the origin and also for the exchange screening terms. The dominant contribution to the exchange-screening diagrams at high Z is from the transverse part of the photon propagator in $|\phi\rangle$.

For the core terms, the exchange terms are often more important than the direct terms, and are again dominated by the transverse components at high Z. For multishell ions, the dominant core contributions involve the core s states, with roughly equal contributions from each principle quantum number; the p states can also make small contributions of up to 10%. Note that previous calculations of the core terms [12, 17] considered only the direct terms, and gave quite different results.

Finally, we note that the ratio of self-energy to Uehling effects is very nearly the same for each analogous pair of terms in Table I. For example, for Li-like U the ratio

of the valence self-energy to the Uehling term is -4.1, which is very nearly the same as the ratio of valence exchange terms. The core terms have a slightly smaller ratio, corresponding to the ratio of self-energy to Uehling term for $1s$ states. Such scaling principles are expected to hold insofar as the self-energy and vacuum polarization scale as the normalization of the external wave function at the origin (see Sec. IV).

Tables II–VII give results for selected ions throughout the Li, Na, and Cu isoelectronic sequences. The tables include our screened QED terms combined with previous calculations of correlation and nuclear effects. Experimental values are also given where available. The QED terms for Z values not tabulated may be evaluated from these tables by interpolation.

For the self-energy in these tables, we use a relativistic basis set with $M = 70$ basis functions in both the positive- and negative-energy branches of the spectrum [17]. The errors given on our QED terms are *numerical* errors for the well-defined terms that we calculate, determined by varying the size of the basis set and other numerical parameters. An interesting feature is that quite reasonable numerical accuracy persists even at low Z, where the present self-energy algorithm suffers from del-

icate cancellations of large, spurious, gauge-dependent terms [15, 16]. One should obtain even greater accuracy for low Z through use of the Coulomb gauge instead of the Feynman gauge used here.

Our results agree with the direct screening terms of Cheng, Johnson, and Sapirstein [13] for Cu-like Au, Na-like Pt, and Li-like U within their larger numerical errors. We also agree quite well with the linearized direct screening calculations of Indelicato and Mohr [12] on Li-like U for all but the $2p_{1/2}$ state. A detailed comparison of these calculations is given in [17].

Figures 3–8 show a comparison of our results with experiment. Since the QED screening terms (Fig. 2) scale roughly as Z^3, we have divided the differences between theory and experiment by this factor, so that missing terms in this order should appear as a constant offset. The agreement is generally very good, although the low-Z results for Cu-like ions disagree systematically with experiment, and isolated discrepancies appear elsewhere. The low-Z Cu-like disagreement probably results from uncalculated higher-order correlation, since the discrepancy is somewhat smaller than the third-order Coulomb energy, the highest-order term in the RMBPT calculation [6]. The correlation is adequately converged for the Li

TABLE I. QED perturbation theory for Li-like U and Na-like Pt. RMBPT, relativistic many-body perturbation theory; SE, self-energy; Uehl., Uehling term; WK, Wichmann-Kroll terms; HO, higher-order two-loop radiative corrections. Units are eV.

Term	Figure	Li-like U $2p_{1/2}$-$2s$	Na-like Pt $3p_{3/2}$-$3s$
RMBPT		322.51(9)[a]	658.76[b]
Valence SE	1(a)	$-54.09(1)$	$-6.80(1)$
Valence SE (ex)	2(e)	0.36	0.10
Core SE (dir)	2(i) +2(j)	0.23(1)	
Core SE (ex)	2(l)	$-0.73(2)$	
Total core SE		$-0.51(2)$	-0.09[c]
Total SE		$-54.24(2)$	$-6.79(1)$
Valence Uehl.	1(b)	13.12	1.50
Valence Uehl. (ex)	2(g)	-0.08	-0.02
Core Uehl. (dir)	2(k)	$-0.08(1)$	
Core Uehl. (ex)	2(n)	0.21	
Total core Uehl.		0.12(1)	0.02[d]
WK		-0.60	-0.06
Total vacuum polarization		12.56(1)	1.44
HO		0.01(4)	0.00
Total QED total		280.83(10)	653.41(1)
Experiment		280.59(9)[e]	653.43(5)[f]

[a]Blundell, Johnson, and Sapirstein, Ref. [7], with $-0.08(8)$ eV for nuclear recoil [17], and 0.18(5) eV for nuclear polarization [27].
[b]Johnson, Blundell, and Sapirstein, Ref. [5].
[c]Sum of Figs. 2(i) and 2(l).
[d]Sum of Figs. 2(k) and 2(n).
[e]Schweppe et al., Ref. [1].
[f]Cowan et al., Ref. [2].

TABLE II. QED contributions for the $2s$-$2p_{1/2}$ transition in Li-like ions. SE, valence self-energy, Fig. 1(a); Uehl., valence Uehling term, Fig. 1(b); X, valence external exchange terms, Figs. 2(e) and 2(g); Other, Wichmann-Kroll plus two-loop radiative corrections; C, core QED, Figs. 2(i)–2(l), 2(n); QED, total QED. Units are eV.

Z	SE	Uehl.	X	Other	C	QED	RMBPT	Sum	Expt.
10	−0.0150(5)	0.0007	0.0007	0.0000	−0.0005(1)	−0.0141(5)	15.9026[a]	15.8885(5)	15.8887(2)[b]
12	−0.0300(5)	0.0016	0.0011(1)	0.0000	−0.0009(1)	−0.0282(5)	19.8671[a]	19.8389(5)	19.8390(4)[b]
15	−0.070(1)	0.004	0.002	0.000	−0.002	−0.066(1)	25.878	25.812(1)	25.814(3)[c]
18	−0.139(1)	0.009	0.003	0.000	−0.003	−0.130(1)	31.998	31.868(1)	31.866(1)[b]
20	−0.205(1)	0.014	0.004	0.000	−0.004	−0.191(1)	36.154	35.964(1)	35.962(2)[d]
30	−0.884(2)	0.075	0.012(1)	−0.001	−0.011(1)	−0.810(2)	58.199	57.389(2)	
32	−1.113(2)	0.097	0.014(1)	−0.001	−0.014(1)	−1.016(2)	62.928	61.911(2)	61.902(4)[e]
40	−2.46	0.25	0.03	0.00	−0.03	−2.22	83.25	81.04	
42	−2.93	0.31	0.03	−0.01	−0.03	−2.63	88.74	86.12	86.10(1)[e]
50	−5.45	0.65	0.05	−0.02	−0.05	−4.81(1)	112.73	107.92(1)	
54	−7.18	0.92	0.06	−0.02	−0.06(1)	−6.29(1)	126.13	119.84(1)	119.97(10)[f]
60	−10.52	1.48	0.08	−0.04(1)	−0.08(1)	−9.08(1)	148.37	139.29(1)	
70	−18.57	3.08	0.13(1)	−0.11(1)	−0.14(1)	−15.61(2)	192.17	176.56(2)	
80	−30.91	6.07	0.19(1)	−0.24(2)	−0.23(2)	−25.12(3)	246.11	220.99(3)	
90	−49.44	11.57	0.25(1)	−0.49(4)	−0.35(3)	−38.45(5)	309.17	270.72(5)	
92	−54.09	13.12	0.27(1)	−0.59(4)	−0.38(3)	−41.68(5)	322.51(9)[g]	280.83(10)	280.59(9)[h]

[a]Terms from [4] recalculated according to [5].
[b]B. Edlén, Phys. Scr. **28**, 51 (1983).
[c]W. C. Martin, R. Zalubas, and A. Musgrove, J. Phys. Chem. Ref. Data **14**, 751 (1985).
[d]J. Sugar and C. Corliss, J. Phys. Chem. Ref. Data **14**, Suppl. No. 2 (1985).
[e]H. Hinnov et al., Phys. Rev. A **40**, 4357 (1989).
[f]S. Martin et al., Europhys. Lett. **10**, 645 (1989).
[g]Includes −0.08(8) eV from nuclear recoil [17], and 0.18(5) eV from nuclear polarization [27].
[h]J. Schweppe et al., Ref. [1].

and Na sequences, where the third-order Coulomb term becomes comparable to the experimental error roughly at the lowest-Z values tabulated. The theory for Na-like Sn $3s$-$3p_{1/2}$ is four experimental standard deviations smaller than the measurement, and the theory for a group of high-Z Cu-like measurements is also system-

atically smaller than the measurements. These discrepancies have also been noted by Kim et al. [31] in their recent very complete study of Li-like, Na-like, and Cu-like ions. These authors took relativistic correlation energies derived from the RMBPT calculations [4–7] together with phenomenological estimates of the QED ef-

TABLE III. QED contributions for the $2s$-$2p_{3/2}$ transition in Li-like ions. Acronyms are defined in the caption to Table II. Units are eV.

Z	SE	Uehl.	X	Other	C	QED	RMBPT	Sum	Expt.
10	−0.0145(5)	0.0007	0.0007	0.0000	−0.0005(1)	−0.0135(5)	16.1066[a]	16.0931(5)	16.0932(2)[b]
12	−0.0289(5)	0.0016	0.0012(1)	0.0000	−0.0009(1)	−0.0269(5)	20.3593[a]	20.3324(5)	20.3318(4)[b]
15	−0.067(1)	0.004	0.002	0.000	−0.002	−0.062(1)	27.267	27.205(1)	27.206(3)[b]
18	−0.132(1)	0.009	0.004	0.000	−0.002	−0.122(1)	35.161	35.039(1)	35.037(1)[b]
20	−0.193(1)	0.014	0.005	0.000	−0.003	−0.178(1)	41.206	41.028(1)	41.029(2)[b]
30	−0.822(2)	0.075	0.014(1)	−0.001	−0.009(1)	−0.743(2)	87.777	87.033(2)	
32	−1.032(2)	0.099	0.016(1)	−0.002	−0.010(1)	−0.929(2)	101.984	101.055(2)	101.043(12)[c]
40	−2.27	0.25	0.03	−0.01	−0.02	−2.00	185.12	183.12	
42	−2.69	0.31	0.03	−0.01	−0.02	−2.37	214.37	211.99	211.94(7)[c]
50	−5.00	0.67	0.05	−0.02	−0.02	−4.31	379.00	374.68	
54	−6.59	0.95	0.07	−0.03	−0.03	−5.62	497.84	492.22	492.34(62)[d]
60	−9.68	1.56	0.09	−0.05(1)	−0.03	−8.11(1)	737.31	729.20(1)	
70	−17.32	3.33	0.14(1)	−0.12(1)	−0.03(2)	−13.99(2)	1359.55	1345.56(2)	
80	−29.56	6.81	0.21(1)	−0.28(2)	0.00(2)	−22.82(3)	2393.15	2370.32(3)	
90	−49.26	13.62	0.32(2)	−0.61(4)	0.06(2)	−35.87(4)	4060.98	4025.10(4)	

[a]Terms from [4] recalculated according to [5].
[b]B. Edlén, Phys. Scr. **28**, 51 (1983).
[c]H. Hinnov et al., Phys. Rev. A **40**, 4357 (1989).
[d]T. E. Cowan et al., Ref. [2].

TABLE IV. QED contributions for the $3s$-$3p_{1/2}$ transition in Na-like ions. Acronyms are defined in the caption to Table II. Units are eV.

Z	SE	Uehl.	X	Other	C	QED	RMBPT	Sum	Expt.
20	−0.0288(4)	0.0019	0.0014(1)	0.0000	−0.0024(2)	−0.0279(5)	21.6277	21.5998(5)	21.5997(4)[a]
30	−0.167(1)	0.014	0.005	0.000	−0.008(1)	−0.157(1)	43.182	43.025(1)	43.024(1)[a]
40	−0.536(1)	0.054	0.011(1)	−0.001	−0.018(2)	−0.491(2)	65.994	65.503(2)	65.504(3)[a]
50	−1.27	0.15	0.02	0.00	−0.03	−1.14	90.85	89.71	89.75(1)[b]
64	−3.28	0.49	0.05	−0.02	−0.07(1)	−2.83(1)	130.76	127.94(1)	
78	−7.08	1.33	0.08	−0.05	−0.14(1)	−5.85(1)	179.36	173.51(1)	
80	−7.82	1.52	0.09	−0.06	−0.14(1)	−6.41(2)	187.19	180.78(2)	
82	−8.63	1.74	0.10	−0.07	−0.15(2)	−7.01(2)	195.28	188.27(2)	
90	−12.58(1)	2.93	0.13(1)	−0.12	−0.21(2)	−9.86(2)	229.84	219.98(2)	

[a] J. Reader et al., J. Opt. Soc. Am. B 4, 1821 (1987).
[b] J. F. Seely et al., At. Data Nucl. Data Tables 47, 1 (1991).

TABLE V. QED contributions for the $3s$-$3p_{3/2}$ transition in Na-like ions. Acronyms are defined in the caption to Table II. Units are eV.

Z	SE	Uehl.	X	Other	C	QED	RMBPT	Sum	Expt.
20	−0.0275(4)	0.0019	0.0014(1)	0.0000	−0.0022(2)	−0.0264(5)	22.2554	22.2290(5)	22.2289(4)[a]
30	−0.156(1)	0.014	0.005	0.000	−0.008(1)	−0.145(1)	48.507	48.362(1)	48.361(2)[a]
40	−0.497(1)	0.055	0.011(1)	−0.001(1)	−0.016(2)	−0.449(2)	87.244	86.795(2)	86.800(6)[a]
50	−1.18	0.16	0.02	0.00	−0.03	−1.03	151.00	149.97	149.98(3)[b]
64	−3.06	0.52	0.05	−0.02	−0.05	−2.55(1)	319.57	317.01(1)	317.30(16)[b]
78	−6.80	1.50	0.09	−0.06	−0.07(1)	−5.34(1)	658.76	653.41(1)	653.43(5)[c]
80	−7.56	1.73	0.09	−0.07	−0.07(1)	−5.88(1)	728.55	722.67(1)	
82	−8.40	2.00	0.10(1)	−0.08	−0.08(1)	−6.46(1)	805.22	798.76(1)	798.65(18)[d]
90	−12.69(1)	3.52	0.13(1)	−0.16	−0.08(1)	−9.28(1)	1193.72	1184.44(1)	

[a] J. Reader et al., J. Opt. Soc. Am. B 4, 1821 (1987).
[b] J. F. Seely et al., At. Data Nucl. Data Tables 47, 1 (1991).
[c] T. E. Cowan et al., Ref. [2].
[d] A. Simionovici, D. D. Dietrich, R. Keville, T. Cowan, P. Beiersdorfer, M. H. Chen, and S. A. Blundell (unpublished).

TABLE VI. QED contributions for the $4s$-$4p_{1/2}$ transition in Cu-like ions. Acronyms are defined in caption to Table II. Units are eV.

Z	SE	Uehl.	X	Other	C	QED	RMBPT	Sum	Expt.
40	−0.0776(4)	0.0075	0.0014(1)	−0.0003	−0.0047(5)	−0.0736(6)	25.5010	25.4273(6)	25.4418(4)[a]
50	−0.255(1)	0.031	0.006	−0.001	−0.012(1)	−0.231(2)	45.129	44.898(2)	44.906(1)[b]
60	−0.613(1)	0.086	0.012(1)	−0.003	−0.023(2)	−0.541(3)	66.097	65.556(3)	65.562(1)[b]
70	−1.24	0.20	0.02	−0.01	−0.04	−1.06	89.02	87.96	87.97(1)[c]
74	−1.59	0.28	0.02	−0.01	−0.05	−1.34	98.89	97.54	97.63(1)[d]
82	−2.50	0.50	0.03	−0.02	−0.07(1)	−2.05(1)	120.05	118.01(1)	118.15(2)[e]
83	−2.63	0.54	0.04	−0.02	−0.07(1)	−2.15(1)	122.84	120.69(1)	120.90(2)[e]
90	−3.76	0.88	0.04	−0.04	−0.10(1)	−2.98(1)	143.30	140.32(1)	
92	−4.15	1.00	0.05	−0.04	−0.10(1)	−3.25(1)	149.45	146.20(1)	146.39(37)[c]

[a] J. Reader and N. Acquista, J. Opt. Soc. Am. 69, 1659 (1979).
[b] J. Reader, N. Acquista, and D. Cooper, J. Opt. Soc. Am. 73, 1765 (1983).
[c] D. R. Kania et al., J. Opt. Soc. Am. B 7, 1993 (1990).
[d] J. F. Seely, C. M. Brown, and W. E. Behring, J. Opt. Soc. Am. B 6, 3 (1989).
[e] J. F. Seely et al., Ref. [3].

TABLE VII.   QED contributions for the $4s$-$4p_{3/2}$ transition in Cu-like ions. Acronyms are defined in the caption to Table II. Units are eV.

Z	SE	Uehl.	X	Other	C	QED	RMBPT	Sum	Expt.
40	−0.0728(4)	0.0077	0.0014(1)	−0.0003	−0.0042(4)	−0.0682(6)	28.2812	28.2130(6)	28.2222(4)[a]
50	−0.237(1)	0.032	0.006	−0.001	−0.010(1)	−0.210(1)	56.823	56.613(1)	56.616(1)[b]
60	−0.571(1)	0.091	0.012(1)	−0.003	−0.018(2)	−0.489(2)	98.947	98.458(2)	98.463(4)[b]
70	−1.17	0.22	0.02	−0.01	−0.03	−0.96	164.39	163.43	163.47(4)[c]
74	−1.51	0.31	0.03	−0.02	−0.03	−1.22	200.11	198.88	198.99(5)[d]
82	−2.43	0.58	0.04	−0.02	−0.04	−1.88	294.42	292.55	292.65(10)[e]
83	−2.57	0.62	0.04	−0.03	−0.04	−1.98	308.81	306.84	306.94(11)[f]
90	−3.79	1.05	0.05	−0.05	−0.04	−2.78	430.00	427.21	427.68(22)[f]
92	−4.23	1.22	0.05	−0.05	−0.04	−3.05(1)	472.27	469.22(1)	469.53(25)[c]

[a] J. Reader and N. Acquista, J. Opt. Soc. Am. **69**, 1659 (1979).
[b] J. Sugar *et al.*, J. Opt. Soc. Am. (to be published).
[c] D. R. Kania *et al.*, J. Opt. Soc. Am. B **7**, 1993 (1990).
[d] J. F. Seely, C. M. Brown, and W. E. Behring, J. Opt. Soc. Am. B **6**, 3 (1989).
[e] J. F. Seely, C. M. Brown, and U. Feldman, At. Data Nucl. Data Tables **43**, 145 (1989).
[f] J. F. Seely *et al.*, Ref. [3].

fects, and made a smoothed fit to the resulting difference between theory and experiment. Our theory is in very good agreement with their smoothed predictions. We refer the reader to this work for a thorough discussion of the trends in the available experimental data.

We also agree with the $2p_{3/2}$-$2p_{1/2}$ splitting measured by Simionovici *et al.* [32], who found 372.15 ± 0.50 eV to be compared with our theoretical value 372.38(1) eV from Tables II and III.

To give some idea of the role of external exchange screening in these calculations, Figs. 3–8 also show the values that would result if exchange screening terms (valence and core) were omitted. For the Li and Na sequences, a trend appears in which theory is systematically larger than experiment; for the Cu sequence, the results at low Z no longer tend to experiment at medium Z. Inclusion of the external exchange screening improves agreement to within one to two experimental standard deviations for the Li and Na sequences. A similar systematic disagreement between theory and experiment would result if core terms were omitted.

It is also interesting to compare our *ab initio* calculation with other estimates of QED effects. Figure 9 shows a comparison of QED theories for the $2s$-$2p_{1/2}$ transition in low-Z Li-like ions, including the QED from the "Welton method" [30] and the "ρ method" [31]. Also shown is the "extended Kabir-Salpeter" result of McKenzie and Drake [33]. All calculations agree at the level of experimental error. Similarly good agreement is found with the Welton and ρ methods for Na-like and Cu-like transitions [31]. Since these methods clearly give some insight into the QED screening mechanism, we examine them in more detail in the next section.

IV. DISCUSSION OF THE SCREENING EFFECT

To investigate the accuracy of phenomenological approaches, we compare calculations of the self-energy in a local model screening potential with phenomenological calculations for the same model potential (the direct part of the V^{N-1} Dirac-Fock potential). We consider the "screening correction" $\Delta E(Z) = E_{\text{ion}}(Z) - E_{\text{hyd}}(Z)$, defined as the difference between the self-energy of a many-electron ion and that of the hydrogenic ion with the same finite nucleus. Phenomenological values for ΔE can be obtained by multiplying Mohr's hydrogenic result [8, 9], corrected for finite nuclear size [28], by various screening factors. If the screened self-energy scales as the relativistic normalization N at the origin, we would have

$$\Delta E_{\text{norm}} = (N_{\text{ion}}/N_{\text{hyd}} - 1)E_{\text{hyd}}. \tag{3}$$

This scaling assumes that the self-energy operator is localized near the origin, and is a function of the nuclear charge Z only. A normalization scaling is made in one of the QED terms, $\Delta E_{L,1}$, in the "extended Kabir-Salpeter" approach of Drake and collaborators [34, 33]. These authors use nonrelativistic probability densities, however, and add the leading correction to this procedure in the $1/Z$ expansion, as well as other QED terms to lowest order in $Z\alpha$. The procedure in (3) is also quite close to the ρ method of Kim *et al.* [31], in which relativistic point-nucleus wave functions are integrated over a small region of space around the nucleus.

Another approximation method is the "Welton method" of Indelicato, Gorceix, and Desclaux [35, 30], which assumes

$$\Delta E_{\text{Welt}} = \left(\langle\nabla^2 V_{\text{ion}}\rangle / \langle\nabla^2 V_{\text{hyd}}\rangle - 1\right) E_{\text{hyd}}. \tag{4}$$

This form follows from the leading term in the nonrelativistic limit of the self-energy [36–38]. Since $\nabla^2 V(r)$ is proportional to the charge density, this estimate is very close to the normalization estimate when the nuclear charge density dominates. However, the electron screen-
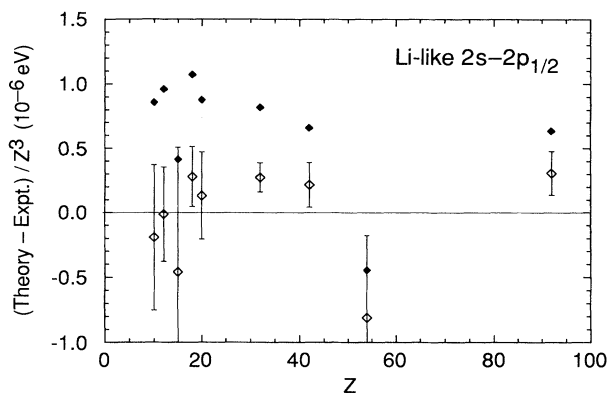
FIG. 3.   Scaled differences between theory and experiment for $2s$-$2p_{1/2}$ transition frequencies in selected Li-like ions. Open diamonds with experimental error bars indicate the complete theory; full diamonds indicate the theory with *external* exchange terms omitted.
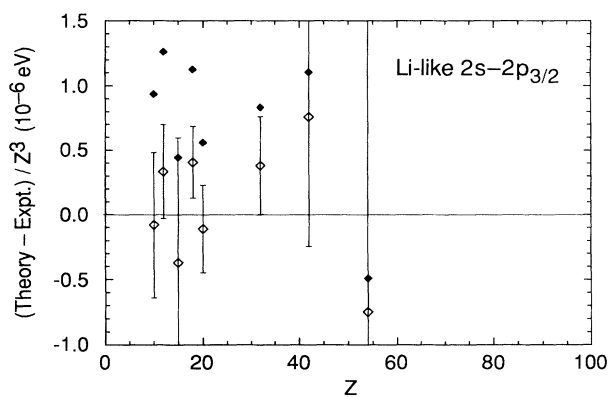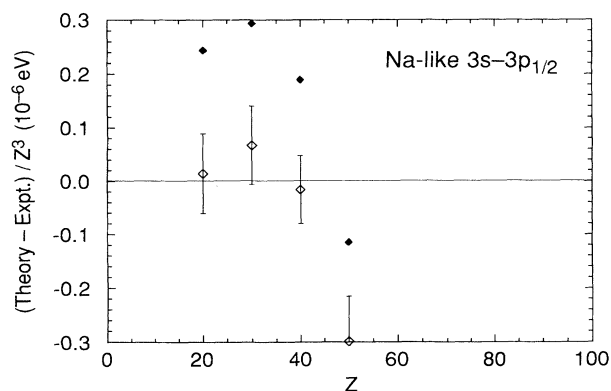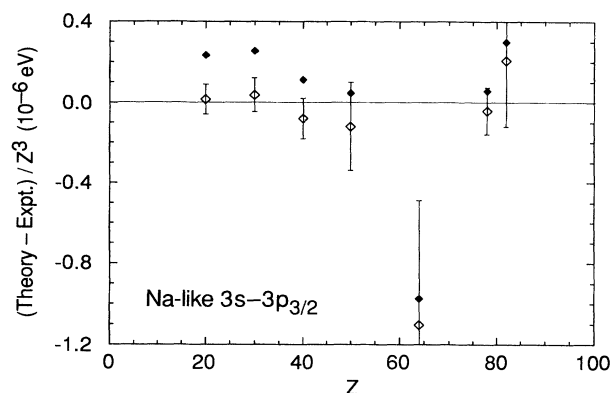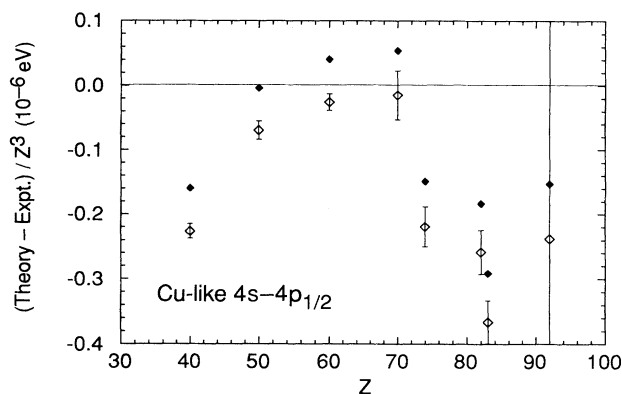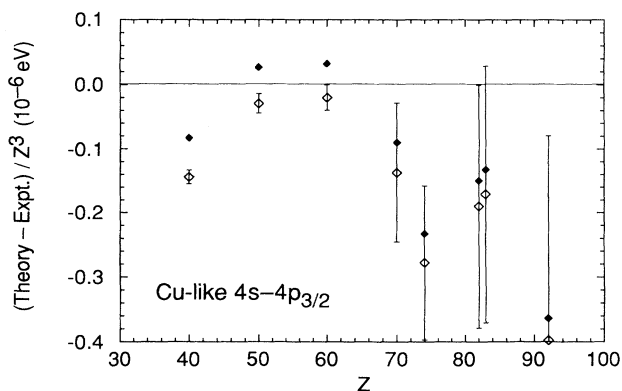

FIG. 6.   Theory minus experiment for $3s$-$3p_{3/2}$ transition frequencies in selected Na-like ions. See the caption to Fig. 3.

FIG. 4.   Theory minus experiment for $2s$-$2p_{3/2}$ transition frequencies in selected Li-like ions. See the caption to Fig. 3.

FIG. 7.   Theory minus experiment for $4s$-$4p_{1/2}$ transition frequencies in selected Cu-like ions. See the caption to Fig. 3.
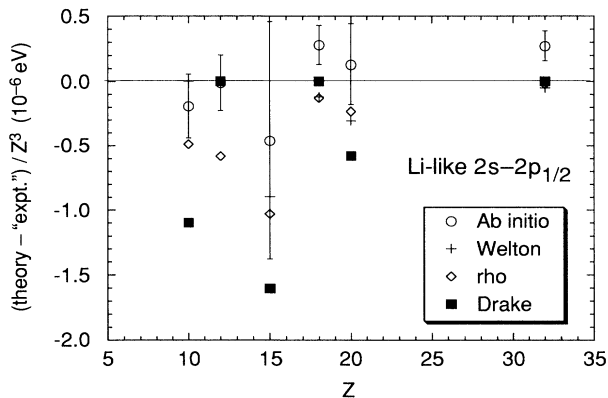

FIG. 5.   Theory minus experiment for $3s$-$3p_{1/2}$ transition frequencies in selected Na-like ions. See the caption to Fig. 3.

FIG. 8.   Theory minus experiment for $4s$-$4p_{3/2}$ transition frequencies in selected Cu-like ions. See the caption to Fig. 3.

FIG. 9. Comparison between various theories (see text) for QED effects in the $2s$-$2p_{1/2}$ transition of Li-like ions. The "experimental" QED value, defined to be the difference between experiment and the RMBPT calculation [4], is subtracted from all values. The error bars shown on one set of points are experimental errors.

ing charge density also contributes an extended operator that makes a small contribution.

Finally, Indelicato, Gorceix, and Desclaux have proposed using the "$g - 2$" term in the self-energy [36] for states with $l \geq 1$,

$$\Delta E_{g-2} = (\langle \beta \boldsymbol{\alpha} \cdot \boldsymbol{\nabla} V_{\text{ion}} \rangle / \langle \beta \boldsymbol{\alpha} \cdot \boldsymbol{\nabla} V_{\text{hyd}} \rangle - 1) E_{\text{hyd}}. \quad (5)$$

Since the expectation value here involves a product of the upper- and lower-component radial functions, the estimate is also quite close numerically to the normalization method.

Figure 10 shows the screening correction for a $2s$ state in Li-like ions. At low Z, our *ab initio* calculation agrees within numerical error with the Welton estimate from (4) for the model potential. The two methods deviate at high Z, however, by about three experimental standard deviations [1] at $Z = 92$.

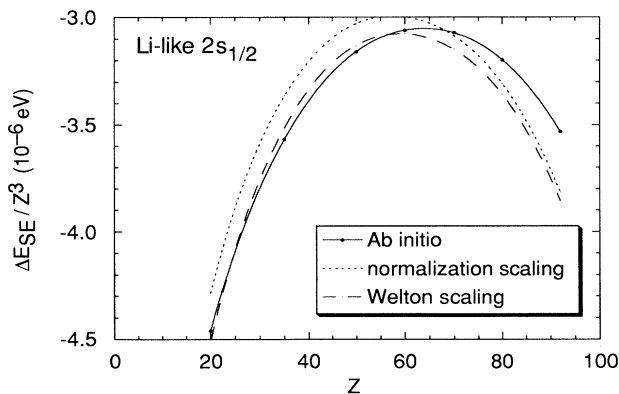A similar analysis is presented in Fig. 11 for the $2p_{1/2}$

FIG. 10. The scaled screening correction to the self-energy of the valence $2s$ state in Li-like ions, calculated by the *ab initio* method of this paper, and by two phenomenological methods.
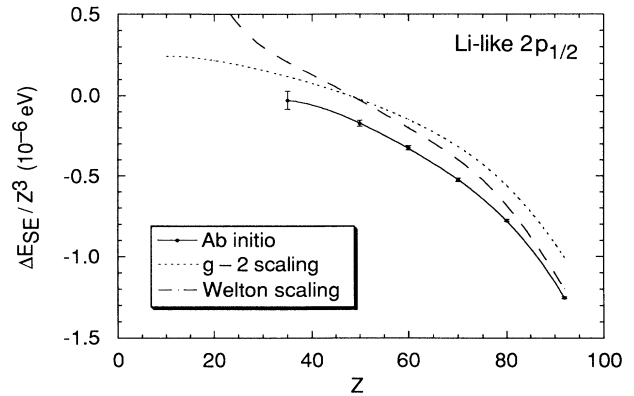
state. We lose numerical control over the calculation for $Z < 35$, but our *ab initio* result appears to follow the "$g - 2$" result at low Z. (The $2p_{1/2}$ screening correction is in any case smaller than the experimental error for $Z < 35$.) For $Z > 80$, the Welton estimate gives closer agreement. This is presumably due to the growth with Z of the probability density at the origin, which vanishes for $p_{1/2}$ states as $Z \rightarrow 0$. The deviation between the *ab initio* and the "$g - 2$" result at $Z = 92$ is about two experimental standard deviations.

Table VIII shows results for low-Z transitions. Our calculated hydrogenic values agree with those of Mohr [9] (the nuclear-finite-size correction present in our result is negligible). Furthermore, we find excellent agreement with the Welton prediction for our model potential in the screened case. For low and medium Z, the external exchange screening terms also scale closely with the change in normalization at the origin when the nonlocal exchange part of the V^{N-1} Dirac-Fock potential is added to the valence Hamiltonian.

In conclusion, then, the phenomenological methods give excellent agreement with *ab initio* calculations, although caution is required for the most precise work at high Z. We note finally that the "$\langle r \rangle$ method," which is the default screening algorithm in the GRASP computer code [39], gives predictions for one-valence-electron systems in significant disagreement with experiment, as is evident from the plots in [31].

FIG. 11. As for Fig. 10 but for the $2p_{1/2}$ state.

TABLE VIII. Calculations of the valence self-energy correction to the $2s$-$2p_{1/2}$ transition of H-like and Li-like ions. The "phenomenological" estimate for Li-like ions uses the Welton method with the potential the same as that used in the *ab initio* calculation. Units are eV.

Z	E_{SE} (H-like) Present	E_{SE} (H-like) Mohr[a]	E_{SE} (Li-like) *ab initio*	E_{SE} (Li-like) Phenom.
10	$-0.0214(5)$	$-0.0211(1)$	$-0.0150(5)$	-0.0148
20	$-0.243(1)$	-0.242	$-0.205(1)$	-0.204

[a]P. J. Mohr, Ref. [9].

V. CONCLUSIONS

We have seen that the combination of the RMBPT terms with the subset of QED terms considered here provides a very complete *ab initio* description of Li-like, Na-like, and Cu-like spectra, generally reproducing the experimental data within one or two experimental standard deviations, apart from the Cu-like sequence at low Z. Although this agreement is good, it should be emphasized that the evaluation of two-photon QED effects is incomplete. The missing effects can be classified into three broad categories: (i) QED screening diagrams, that is, the omitted internal exchange-screening diagrams; (ii) QED effects contained in correlation-type diagrams, omitted in the approximate RMBPT evaluation of these diagrams; (iii) two-loop radiative corrections (also present in hydrogenic systems). In category (ii) we include in particular effects associated with the two-photon box and crossed-box diagrams, specifically Breit-Breit terms, retardation terms, and effects associated with virtual negative-energy electron states. It is important to evaluate all these missing QED effects because by power-counting arguments they enter in the same nominal order, $(Z\alpha)^3$ Ry, as the QED screening effects evaluated here. This applies to the terms in (i), and to some of those in (ii). The two-loop radiative corrections (iii) enter in order $(Z\alpha)^4$ Ry, and may also be important at high Z.

An important empirical result of this paper is that, in spite of the incomplete treatment of two-photon QED effects, the calculation appears to account well for QED effects at the level of experimental error, at least for the Li and Na sequences. The implication is that the omitted QED terms are either separately small at the level of experimental error, or else that they are larger but happen to cancel throughout each isoelectronic sequence. We speculate that the former situation may hold.

This speculation is based on the following arguments. An estimate of two-loop radiative corrections (iii), based on the lowest-order terms in $Z\alpha$ [28–30], appears as HO in Table I, and as part of the column "Other" in Tables II–VII. These contributions are small, less than or comparable to an experimental error for all transitions considered. The omitted higher-order terms in $Z\alpha$ should be of the same order of magnitude or less. As to the effects in category (ii), one may make the following order-of-magnitude estimates, which suggest that they may also be small. The effect of virtual negative-energy states has been estimated for $1s$ states by Sapirstein [40]; estimates for other principal quantum numbers follow by scaling according to the probability density at the origin. The Breit-Breit terms may be estimated as $(Z\alpha)^2$ times the Breit-Coulomb terms given in Refs. [4–7]. The omitted retardation terms, by power-counting arguments, are comparable to or smaller than the Breit-Breit terms. In each case, the resulting estimates are comparable to or smaller than the experimental error for all transitions.

This leaves the internal exchange screening terms of category (i), which are hard to estimate and nominally enter at the same level as the calculated external exchange effects. However, it is not unreasonable to suppose they may be small through the following argument. There is some degree of analogy between the direct diagrams in Figs. 2(a) and 2(b) and the exchange diagrams of Figs. 2(e) and 2(f), because in the former an additional potential is inserted into a diagonal matrix element of the self-energy, and in the latter into an off-diagonal element. Our calculations show the internal direct effect 2(b) to be a small fraction, (5–20)%, of the external direct effect 2(a). The dominance of external effects for direct terms partly explains the close dependence of screening corrections on the normalization at the origin, since this scaling considers just the modification of the external wave function. If external terms dominate for the exchange diagrams as well, this could explain the observed agreement with experiment.

The situation for Li-like U deserves special consideration because of the high accuracy of that measurement. The small size of the two-loop radiative corrections (HO term) in Table I results from cancellations between terms of order 0.5σ, where σ is an experimental standard deviation. The omitted higher-order terms in $Z\alpha$ may enter at a similar level; this possibility is allowed for by the error in parentheses in the table. The estimates above for the omitted terms of category (ii) are for this transition comparable to an experimental standard deviation. As to the internal exchange effects, a conservative estimate is that they may be of the same order as the external exchange effects, which reach 8σ for the core terms; taking 20% of the external exchange terms still gives a $(1–2)\sigma$ effect. Thus, the present 2.5σ discrepancy between theory and experiment is entirely reasonable pending evaluation of the remaining two-photon QED terms.

Perhaps the best way at present to address the possible problem of convergence of RMBPT at low Z for Cu-like systems is to use relativistic all-order procedures such as described in [41] or [42]. While these procedures do not pick up the entire fourth-order Coulomb interaction in a strict perturbative sense, they do sum infinite subsets of diagrams that are known to be dominant in neutral alkali-metal atoms [43,44] or the infinite electron gas [45].

As to the remaining two-photon QED effects, we believe they can all be evaluated by relativistic basis-set methods similar to those used in the RMBPT method and in the self-energy algorithm for this work. The completion of this program should permit a rigorous QED evaluation of the structure of high-Z ions at the 0.1-eV level.

APPENDIX: OFF-DIAGONAL SELF-ENERGY

Consider the general off-diagonal matrix element of the self-energy plus the corresponding matrix element of the

mass counterterm,

$$\Delta E = \langle A|\gamma_0\Sigma(\varepsilon_A)|\phi\rangle - \langle A|\gamma_0\delta m|\phi\rangle . \qquad \text{(A1)}$$

Here $|A\rangle$ is a single-particle state in a potential $V(r)$; its eigenvalue ε_A forms the evaluation energy of the bound-state self-energy operator Σ for $V(r)$. The state $|\phi\rangle$ is completely general. To investigate the cancellation of divergences, we decompose Σ into zero-, one-, and many-potential terms according to the number of potentials appearing in the internal electron propagator [46, 15]

$$\Sigma(\varepsilon_A) = \Sigma^{(0)}(\varepsilon_A) + \Sigma^{(1)}(\varepsilon_A) + \Sigma^{(2+)}(\varepsilon_A). \qquad \text{(A2)}$$

Here $\Sigma^{(0)}(\varepsilon_A)$ is just the free-electron self-energy, which in momentum space satisfies

$$\Sigma^{(0)}(\varepsilon_A, \mathbf{p}) = \delta m + (p_A^\mu\gamma_\mu - m)\chi + \Sigma_{\text{fin}}^{(0)}(\varepsilon_A, \mathbf{p}), \qquad \text{(A3)}$$

where $p_A^\mu \equiv (\varepsilon_A, \mathbf{p})$, χ is a divergent wave-function-renormalization constant, and $\Sigma_{\text{fin}}^{(0)}$ is finite. Similarly, $\Sigma^{(1)}(\varepsilon_A)$ is constructed from the free-electron vertex function Γ^μ and the local potential $A^\mu = (V, \mathbf{0})$. In momentum space,

$$\Sigma^{(1)}(\varepsilon_A\mathbf{p}_2, \varepsilon_A\mathbf{p}_1) = A_\mu(\mathbf{p}_2 - \mathbf{p}_1)\Gamma^\mu(\varepsilon_A\mathbf{p}_2, \varepsilon_A\mathbf{p}_1), \qquad \text{(A4)}$$

with

$$\Gamma^\mu(\varepsilon_A\mathbf{p}_2, \varepsilon_A\mathbf{p}_1) = -\chi\gamma^\mu + \Gamma_{\text{fin}}^\mu(\varepsilon_A\mathbf{p}_2, \varepsilon_A\mathbf{p}_1), \qquad \text{(A5)}$$

where $\Gamma_{\text{fin}}^\mu(\varepsilon_A\mathbf{p}_2, \varepsilon_A\mathbf{p}_1)$ is finite. The many-potential part $\Sigma^{(2+)}(\varepsilon_A)$ of the self-energy is finite.

After substituting (A2)–(A5) into (A1) and using the identity

$$\langle A|\gamma_0(p_A^\mu\gamma_\mu - m)|\phi\rangle = \langle A|(\varepsilon_A - \boldsymbol{\alpha}\cdot\mathbf{p} - \beta m)|\phi\rangle$$
$$= \langle A|V|\phi\rangle, \qquad \text{(A6)}$$

the terms involving the divergent constants δm and χ cancel leaving

$$\Delta E = \langle A|\gamma_0\Sigma_{\text{fin}}^{(0)}(\varepsilon_A)|\phi\rangle + \langle A|\gamma_0\Sigma_{\text{fin}}^{(1)}(\varepsilon_A)|\phi\rangle$$
$$+ \langle A|\gamma_0\Sigma^{(2+)}(\varepsilon_A)|\phi\rangle. \qquad \text{(A7)}$$

Our numerical technique for evaluating this expression follows a simple generalization of that described in [17]

for the diagonal self-energy $|\phi\rangle = |A\rangle$.

The energy shift from Fig. 2(e) satisfies

$$\Delta E^{(e)} = 2\,\text{Re}\,\langle v|\gamma_0[\Sigma(\varepsilon_v) - \delta m]|\phi\rangle, \qquad \text{(A8)}$$

where, after angular reduction,

$$|\phi\rangle = -\sum_{\substack{i,v \\ (i\neq v)}}\sum_{c,L}|i\rangle\frac{R_L(\varepsilon_v - \varepsilon_c; iccv)}{\varepsilon_v - \varepsilon_i}\Delta(j_c, L, j_v)$$
$$\times\frac{(-1)^{j_c+L-j_v}}{2j_v + 1}\delta(\kappa_i, \kappa_v), \qquad \text{(A9)}$$

with $R_L(\omega; abcd)$ a generalized frequency-dependent Slater integral given in Feynman gauge in [17]. The symbol $\Delta(j_c, L, j_v)$ is unity if the three angular momenta satisfy a triangular condition, and zero otherwise. The factor of 2 in (A8) caters for the mirror-image diagram.

Likewise, the core term Fig. 2(l) satisfies

$$\Delta E^{(l)} = 2\,\text{Re}\sum_{c\,(\text{core})}\langle c|\gamma_0[\Sigma(\varepsilon_c) - \delta m]|\phi_c\rangle, \qquad \text{(A10)}$$

$$|\phi_c\rangle = -\sum_{i\,(\neq c)}\sum_L|i\rangle\frac{R_L(\varepsilon_v - \varepsilon_c; ivvc)}{\varepsilon_c - \varepsilon_i}\Delta(j_c, L, j_v)$$
$$\times\frac{(-1)^{j_c+L-j_v}}{2j_v + 1}\delta(\kappa_i, \kappa_v). \qquad \text{(A11)}$$

The exchange-screening terms for the vacuum polarization are evaluated as off-diagonal matrix elements of the Uehling potential with the same states $|\phi\rangle$ above.

In evaluating Σ and $|\phi\rangle$, we take $V(r) = V_{\text{nuc}}(r) + V_{\text{DF,dir}}(r)$ for valence terms, and $V(r) = V_{\text{nuc}}(r) + V_{\text{DF,dir}}(r) - V_c(r)$ for core terms, where c is the core state under consideration in the sum over c in (A10), and where

$$V_c(r) = \int_0^\infty dr'\frac{1}{r_>}[g_c^2(r) + f_c^2(r)], \qquad \text{(A12)}$$

and $g_c(r)$ and $f_c(r)$ are radial eigenstates for the V^{N-1} Dirac-Fock potential. The inclusion of $V_c(r)$ corresponds to a small approximate higher-order term that removes a spurious self-interaction between the core state c and itself.

Finally, we consider the gauge dependence of the expression (A1). The self-energy matrix element can be written (with $k^2 \equiv k_0^2 - \mathbf{k}^2$),

$$\langle A|\gamma_0\Sigma(\varepsilon_A)|\phi\rangle = i\alpha\int\frac{d^4k}{(2\pi)^4}\frac{\Delta^{\mu\nu}(k)}{k^2 + i\delta}\sum_i\frac{\langle A|\alpha_\mu e^{-i\mathbf{k}\cdot\mathbf{r}}|i\rangle\langle i|\alpha_\nu e^{i\mathbf{k}\cdot\mathbf{r}}|\phi\rangle}{\varepsilon_A + k_0 - \varepsilon_i \pm i\delta} , \qquad \text{(A13)}$$

where we have used the momentum-space representation of the photon propagator,

$$D^{\mu\nu}(k_0; \mathbf{r}_2, \mathbf{r}_1) = \int\frac{d^3k}{(2\pi)^3}\frac{\Delta^{\mu\nu}(k)}{k^2 + i\delta}e^{i\mathbf{k}\cdot(\mathbf{r}_2-\mathbf{r}_1)} , \qquad \text{(A14)}$$

and the spectral decomposition of the electron propagator. In the exponential $e^{i\mathbf{k}\cdot\mathbf{r}}$ in (A13), $\mathbf{r}$ is the position operator, and the momentum $\mathbf{k}$ is a parameter. The quantity $\Delta^{\mu\nu}(k)$ is gauge dependent,

$$\Delta^{\mu\nu}(k) = \begin{cases} -g^{\mu\nu} & \text{(Feynman gauge)} \\ -g^{\mu\nu} + (1 - \lambda)k^\mu k^\nu/k^2 & \text{(General covariant gauge)} \\ -g^{\mu\nu} - k^\mu k^\nu/\mathbf{k}^2 + k_0(k^\mu\eta^\nu + k^\nu\eta^\mu)/\mathbf{k}^2 & \text{(Coulomb gauge)}. \end{cases} \qquad \text{(A15)}$$

In the Coulomb-gauge expression, $\eta^\mu \equiv (1,0,0,0)$. The matrix elements appearing in (A13) satisfy the following useful identities:

$$k^\mu \langle a | \alpha_\mu e^{i\mathbf{k}\cdot\mathbf{r}} | b \rangle = k_0 \langle a | e^{i\mathbf{k}\cdot\mathbf{r}} | b \rangle - \langle a | \boldsymbol{\alpha} \cdot \mathbf{k} e^{i\mathbf{k}\cdot\mathbf{r}} | b \rangle$$
$$= k_0 \langle a | e^{i\mathbf{k}\cdot\mathbf{r}} | b \rangle - \langle a | [h_0, e^{i\mathbf{k}\cdot\mathbf{r}}] | b \rangle$$
$$= (k_0 - \varepsilon_a + \varepsilon_b) \langle a | e^{i\mathbf{k}\cdot\mathbf{r}} | b \rangle , \qquad (A16)$$

and similarly,

$$k^\mu \langle a | \alpha_\mu e^{-i\mathbf{k}\cdot\mathbf{r}} | b \rangle = (k_0 + \varepsilon_a - \varepsilon_b) \langle a | e^{-i\mathbf{k}\cdot\mathbf{r}} | b \rangle . \qquad (A17)$$

These expressions hold only if the reference potential $V(r)$ is local (as in this work), for the use of the commutator in (A16) is valid only in that case.

Now, the extra term $(1 - \lambda) k^\mu k^\nu / k^2$ in $\Delta^{\mu\nu}(k)$ for general covariant gauges leads to the following extra term when substituted in (A13):

$$\Delta E_\lambda = i\alpha(1 - \lambda) \int \frac{d^4 k}{(2\pi)^4} \frac{1}{(k^2)^2} k^\nu \langle A | \alpha_\nu | \phi \rangle . \qquad (A18)$$

We have here used (A17) and completed the sum over i. This term vanishes because the integrand is an odd function of k, showing that the covariant gauges give equal matrix elements for a fixed, arbitrary state $|\phi\rangle$.

The state $|\phi\rangle$ itself is in principle gauge dependent, however. For valence exchange terms, it has the form

$$|\phi\rangle = -\alpha \sum_{i\,(\neq A)} \frac{|i\rangle}{\varepsilon_A - \varepsilon_i} \sum_{c\,(\text{core})} \int \frac{d^3 k}{(2\pi)^3} \frac{\Delta^{\mu\nu}(k)}{k^2 + i\delta} \langle i | \alpha_\nu e^{i\mathbf{k}\cdot\mathbf{r}} | c \rangle \langle c | \alpha_\mu e^{-i\mathbf{k}\cdot\mathbf{r}} | A \rangle , \qquad (A19)$$

with $k_0 \equiv \varepsilon_A - \varepsilon_c$. The extra term $(1 - \lambda) k^\mu k^\nu / k^2$ in $\Delta^{\mu\nu}(k)$ then gives a vanishing contribution by virtue of (A17). A similar conclusion holds for $|\phi_c\rangle$ for core exchange terms. Thus, since the free-electron mass shift δm is gauge invariant, the external exchange terms are seen to be gauge invariant over covariant gauges.

Repeating this discussion for Coulomb gauge, one finds that the second and third terms in $\Delta^{\mu\nu}(k)$ for Coulomb gauge give vanishing terms for the above reasons, but

that the fourth term $k_0 k^\nu \eta^\mu / k^2$ gives a nonvanishing contribution in both (A13) and (A19) (unless $|\phi\rangle = |A\rangle$, which establishes gauge invariance for the diagonal self-energy). The external exchange terms thus have a partial gauge dependence. The explicit Feynman gauge calculation of external terms given here, however, shows that the covariant gauges give results with the expected order of magnitude as well as the expected approximate Z^3 dependence.

[1] J. Schweppe, A. Belkacem, L. Blumenfeld, N. Claytor, B. Feinberg, H. Gould, V. E. Kostroun, L. Levy, S. Misawa, J. R. Mowat, and M. H. Prior, Phys. Rev. Lett. 66, 1434 (1991).

[2] T. E. Cowan, C. L. Bennett, D. D. Dietrich, J. Bixler, C. J. Hailey, J. R. Henderson, D. A. Knapp, M. A. Levine, R. E. Marrs, and M. B. Schneider, Phys. Rev. Lett. 66, 1150 (1991).

[3] J. F. Seely, J. O. Ekberg, C. M. Brown, U. Feldman, W. E. Behring, J. Reader, and M. C. Richardson, Phys. Rev. Lett. 57, 2924 (1986).

[4] W. R. Johnson, S. A. Blundell, and J. Sapirstein, Phys. Rev. A 37, 2764 (1988).

[5] W. R. Johnson, S. A. Blundell, and J. Sapirstein, Phys. Rev. A 38, 2699 (1988).

[6] W. R. Johnson, S. A. Blundell, and J. Sapirstein, Phys. Rev. A 42, 1087 (1990).

[7] S. A. Blundell, W. R. Johnson, and J. Sapirstein, Phys. Rev. A 41, 1698 (1990).

[8] P. J. Mohr, Ann. Phys. (N.Y.) 88, 26 (1974); 88, 52 (1974).

[9] P. J. Mohr, Phys. Rev. Lett. 34, 1050 (1975); Phys. Rev. A 26, 2338 (1982).

[10] P. J. Mohr, Phys. Rev. A 46, 4421 (1992).

[11] P. J. Mohr and Y.-K. Kim, Phys. Rev. A 45, 2727 (1992).

[12] P. Indelicato and P. J. Mohr, in Atomic Physics 12, Proceedings of Papers on Trapping of Neutral Atoms, History of ICAP, and Tests of Symmetries, edited by Jens C. Zorn and Robert R. Lewis, AIP Conf. Proc. No. 233 (AIP, New York, 1990); Theor. Chim. Acta 80, 207 (1991).

[13] K. T. Cheng, W. R. Johnson, and J. Sapirstein, Phys. Rev. Lett. 66, 2960 (1991).

[14] G. E. Brown, J. S. Langer, and G. W. Schaefer, Proc. R. Soc. (London) Ser. A 251, 92 (1959).

[15] N. J. Snyderman, Ann. Phys. (N.Y.) 211, 43 (1991).

[16] S. A. Blundell and N. J. Snyderman, Phys. Rev. A 44, R1427 (1991).

[17] S. A. Blundell, Phys. Rev. A 46, 3762 (1992).

[18] M. Gell-Mann and F. Low, Phys. Rev. 84, 350 (1951).

[19] J. Sucher, Phys. Rev. 107, 1448 (1957).

[20] P. J. Mohr, in Relativistic, Quantum Electrodynamic, and Weak Interaction Effects in Atoms, Proceedings of the Program Held on Relativistic, Quantum Electrodynamic, and Weak Interaction Effects in Atoms at the Institute of Theoretical Physics, Santa Barbara, CA, 1988, edited by W. R. Johnson, P. J. Mohr, and J. Sucher, AIP Conf. Proc. No. 189 (AIP, New York, 1988).

[21] J. Sapirstein, Phys. Scr. 36, 801 (1987).

[22] J. Sucher, Int. J. Quantum Chem. 24, 3 (1984).

[23] E. A. Uehling, Phys. Rev. 48, 55 (1935).

[24] R. Serber, Phys. Rev. 48, 49 (1935).

[25] G. Soff and P. J. Mohr, Phys. Rev. A 38, 5066 (1988).

[26] J. D. Zumbro, E. B. Shera, Y. Tanaka, C. E. Bemis, Jr., R. A. Naumann, M. V. Hoehn, W. Reuter, and R. M. Steffen, Phys. Rev. Lett. 20, 1888 (1984).

[27] G. Plunien, B. Müller, W. Greiner, and G. Soff, Phys. Rev. A 39, 5428 (1989); 43, 5853 (1991).

[28] W. R. Johnson and G. Soff, At. Data Nucl. Data Tables

33, 405 (1985).

[29] T. Beier and G. Soff, Z. Phys. D **8**, 129 (1988).

[30] P. Indelicato and J.P. Desclaux, Phys. Rev. A **42**, 5139 (1990).

[31] Y.-K. Kim, D. H. Baik, P. Indelicato, and J. P. Desclaux, Phys. Rev. A **44**, 148 (1991).

[32] A. Simionovici, D. D. Dietrich, D. Leneman, and J. P. Grandin, Phys. Rev. A **41**, 5250 (1990).

[33] D. K. McKenzie and G. W. F. Drake, Phys. Rev. A **44**, R6973 (1991).

[34] S. P. Goldman and G. W. F. Drake, J. Phys. B **17**, L197 (1984); G. W. F. Drake, Can. J. Phys. **66**, 586 (1988).

[35] P. Indelicato, O. Gorceix, and J. P. Desclaux, J. Phys. B **20**, 651 (1987).

[36] H. A. Bethe and E. E. Salpeter, *Quantum Mechanics of One- and Two-Electron Atoms* (Plenum, New York, 1977).

[37] J. Dupont-Roc, C. Fabre, and C. Cohen-Tannoudji, J. Phys. B **20**, 651 (1987).

[38] G. Feldman and T. Fulton, Ann. Phys. (N.Y.) **184**, 231 (1988).

[39] I. P. Grant, B. J. McKenzie, P. H. Norrington, D. F. Mayers, and N. C. Pyper, Comput. Phys. Commun. **21**, 207 (1980); B. J. McKenzie, I. P. Grant, and P. H. Norrington, *ibid.* **21**, 233 (1980).

[40] J. Sapirstein, in *Relativistic, Quantum Electrodynamic, and Weak Interaction Effects in Atoms*, Proceedings of the Program Held on Relativistic, Quantum Electrodynamic, and Weak Interaction Effects in Atoms at the Institute of Theoretical Physics, Santa Barbara, CA, 1988, edited by W. R. Johnson, P. J. Mohr, and J. Sucher, AIP Conf. Proc. No. 189 (AIP, New York, 1988).

[41] S. A. Blundell, W. R. Johnson, and J. Sapirstein, Phys. Rev. A **40**, 2233 (1989); **43**, 3407 (1991).

[42] S. Salomonson and P. Öster, Phys. Rev. A **41**, 4670 (1990).

[43] V. A. Dzuba, V. V. Flambaum, and O. P. Sushkov, Phys. Lett. **142**, 373 (1989).

[44] S. A. Blundell, W. R. Johnson, and J. Sapirstein, Phys. Rev. A **42**, 3751 (1990).

[45] A. L. Fetter and J. D. Walecka, *Quantum Theory of Many-Particle Systems* (McGraw-Hill, New York, 1971).

[46] M. Baranger, H. A. Bethe, and R. P. Feynman, Phys. Rev. **92**, 482 (1953).